EurJIC
European Journal of Inorganic Chemistry

Research Article
doi.org/10.1002/ejic.202400402

Chemistry Europe
European Chemical Societies Publishing

www.eurjic.org

N-Heterocyclic Carbene Complexes Ru^{II}(Arene) and their Application as ROMP Catalysts, Antioxidant and Anticancer Agents

Rubina Troiano,[a] Domenico Iacopetta,[b] Assunta D'Amato,*[a] Annaluisa Mariconda,[c] Jessica Ceramella,[b] Alessia Catalano,[d] Maria Stefania Sinicropi,[b] and Pasquale Longo[a]

N-Heterocyclic carbenes (NHCs) play an important role in metal complex catalysis and stabilisation, providing stability under non-inert conditions and a high σ-donor capacity. They are crucial ligands for the synthesis of organometallic compounds like Ru^{II}-complexes, which can operate as very active catalysts for a variety of chemical transformations and functionalizations. RA(Ruthenium-arene)NHC complexes, known for their piano-stool structure, stabilise Ru(II) oxidation state by occupying three ruthenium coordination sites with a η^6-coordinated arene ligand. The development of dual-acting Ru^{II}-arene complexes has sparked increased interest in their catalytic and biological properties. Because of their broad spectrum, metal complexes can give distinct mechanisms of pharmacological action from organic drugs. This study aimed to explore the impact of ligand amphiphilicity and counterion on bioactivity, designing a family of compounds with the NHC ligand bearing an ester moiety and switching the wingtip substituent from methyl to benzyl units. All synthesized compounds were tested in norbornene ROMP, a benchmark reaction for Ru^{II} potential catalysts and as anticancer and antioxidant compounds.

Introduction

N-Heterocyclic carbenes (NHCs) today constitute a notable species in catalysis and in stabilization of metal complexes.[1,2] Among the several benefits associated with the use of an NHC ligand, which include stability under non-inert conditions and strong σ-donor capacity, rely the almost endlessly possibilities to tune the steric and electronic properties of the ligand itself by modifications of the heterocycles' substituents. Specifically, they have proven to be incredibly important ligands for the development of organometallic compounds that can be highly active catalysts for an amazing number of chemical transformations and functionalizations,[3–6] among which olefin metathesis.[7–9] Notably, they can frequently be effective drugs capable of acting as anticancer, antimicrobial[10] and antioxidant agents[11,12] as well. Among these compounds, Ru^{II}-complexes have been widely studied since the development of the first and second generations Grubbs' and Hoveyda-Grubbs' catalysts.[13–16] Most synthetic pathways leading to NHC-Ru^{II} complexes classically involve bis(phosphane) benzylidene intermediates;[17,18] however, in recent years, an interesting class of complexes, RANHC, acronym for Ruthenium(II)-Arene-NHC, has been developed. These can be easily accessed either by direct reaction of a stoichiometric amount of free carbene, generated *in situ* by deprotonation of a more stable ionic precursor, and the commercially available Ru dimer [(*p*-cymene)$RuCl_2]_2$,[19,20] or by transmetallation route from a parent silver complex.[21,22] Often related to RAPTA (Ruthenium-Arene-PTA (1,3,5-triaza-7-phosphaadamantane)][23–25] complexes, RANHC are distinguished by their piano-stool structure (Figure 1), which stabilizes the Ru(II) oxidation state by occupying three of the ruthenium coordination sites with an η^6-coordinated arene ligand. The main ligand (ancillary ligand) occupies another coordination site, leaving two other coordination sites free to be filled by typically labile chloride ligands.

The main difference between RAPTA and RANHC relies in the substitution of the amphiphilic phosphine ligand PTA, which was originally introduced to enhance the physiological environment solubility of the resulting complex, with an *N*-

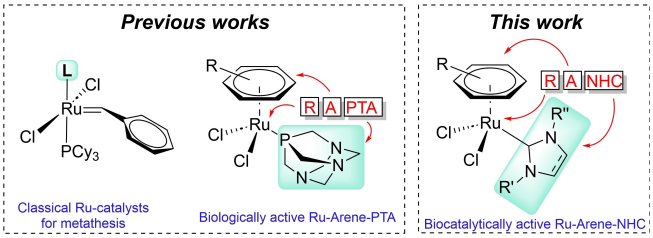

Figure 1. Left to right: Schematic structure of classical Grubbs' and Hoveyda-Grubbs' Ru^{II} precatalysts; schematic structure of Ru^{II}-Arene-PTA; schematic structure of Ru^{II}-Arene-NHC.

[a] *Dr. R. Troiano, Dr. A. D'Amato, Prof. P. Longo*
Department of Chemistry and Biology "A. Zambelli", University of Salerno, Via Giovanni Paolo II, 132, I-84084 Fisciano (SA), Italy
E-mail: asdamato@unisa.it

[b] *Prof. D. Iacopetta, Dr. J. Ceramella, Prof. M. Stefania Sinicropi*
Department of Pharmacy, Health and Nutritional Sciences, University of Calabria, Via P. Bucci, 87036 Arcavacata di Rende, Italy

[c] *Prof. A. Mariconda*
Department of Basic and Applied Sciences, University of Basilicata, Via Dell'Ateneo Lucano 10, 85100 Potenza, Italy

[d] *Prof. A. Catalano*
Department of Pharmacy-Drug Sciences, University of Bari "Aldo Moro", I-70126 Bari, Italy

Supporting information for this article is available on the WWW under https://doi.org/10.1002/ejic.202400402

Research Article
doi.org/10.1002/ejic.202400402

heterocyclic ligand, which has stronger σ-donation and stereo-electronic mouldability (Figure 1).

The past couple of decades have seen an increasing interest in the development of dual-acting Ru^{II}-arene complexes, displaying both catalytic[26] and biological[27] activity.

Possibly, the most famous class of Ru-catalysed reactions involves alkene or alkyne metathesis reactions,[26,28] such as ring-opening metathesis polymerisation (ROMP),[19,20,29–31] ring-closing metathesis (RCM),[32] cross-metathesis[33] or enyne metathesis (EYM), whose outcome is deeply influenced by the ligand constitution.[26,34] Moreover, transformation of small molecules to obtain relevant building blocks, has recently been explored, particularly involving transfer (de)hydrogenation (reduction of double carbon-carbon and carbon-oxygen bonds)[35,36] amine, imine and amide formation.[37–39]

In these regards, the past few decades have been dedicated to the improvement of the catalytic performances of the metal complex by progressive modifications of the ancillary and labile ligands constitution. As far as the stability of the precatalytical complex is concerned, RANHC complexes, when compared to the parent Grubbs' and Hoveyda-Grubbs', display an increased ease of management, as they tend to be oxygen and moisture resistant. Such stability can be further enhanced by the presence of an additional hemilabile group, positioned on one of the peripheral nitrogen moieties.

For example, amine, pyridine,[40] ether[35] and thioether[36] groups have been chelated to Ru^{II}-complexes, promoting stabilization of unsaturated intermediates and thereby improving catalyst stability and efficiency.

Whereas the latter transformations, in which the precatalyst is normally activated by the arene disengagement, followed by the coordination of the substrate, the former, especially ROMP, require the formation of a Ru-alkylidene specie, and are far less studied.

In fact, unlike Grubbs' ruthenium-benzylidene complexes, ruthenium-arene species lack the alkylidene moiety that is essential for enabling metathesis reactions. However, highly active species can be generated *in situ* either thermally,[29,41] photochemically[42] or by arene disengagement in the presence of a carbene activator.[43–48] Noteworthily, these systems are still scarcely studied in the literature, due to unclear mechanisms involving the arene disengagement and monomer coordination. The fundamental disadvantage of this system is the inadequate control over the initiation stage, often resulting in high molecular weights and broad polydispersities. Because few propagating species are present in solution, even minor changes in initiation efficiency can result in substantial differences in the control of molecular weights.

As far as the biological activities are concerned, both Ru^{III} and Ru^{II} complexes are able to exert cytotoxic activity against solid tumors.[27,49]

In fact, metal complexes can provide different mechanisms of drug action compared to organic agents because of their broad range of coordination and oxidation numbers, geometries, and kinetic properties. As a result, there is a growing interest in using metal complexes as pharmaceuticals for chemotherapeutic or diagnostic purposes.

Unsurprisingly, Grubbs type prototypic ruthenium NHC complexes, akin to many organometallic bioactive compounds, exhibit considerable biological effectiveness.[50] Lead compounds have been successfully established, and ruthenium complexes themselves have been playing a dramatically growing role in inorganic medicinal chemistry.[51] As a result, following the revolutionary platinum cytostatic drugs, these transition metal complexes are currently regarded as the second most promising class of novel anticancer metal species. In RAPTA and RANHC prototypes, $RuCl_2$(arene) constitutes the organometallic pharmacophoric core,[52–54] while the phosphine or the carbene *N*-heterocyclic ligand plays a crucial role into the stabilization of the metallic core in the biological environment; efforts have been made to design an NHC imidazol(in)ium moiety capable to infer such kinetic inertness and amphiphilicity.[49,51,55]

The very same complex can display anticancer, antimicrobial and antioxidant properties, furnishing a wide-spectrum bioactivity. In particular, RANHC complexes featuring an imidazolium core, endowed with a (2-methoxy-2-phenyl)ethyl hydrophobic nitrogen substituent (Figure 2, **RuA**–**C**), exhibit strong anticancer action, primarily against MDA-MB-231 breast cancer cells. Also, antibacterial action, especially against *S. aureus*, was observed but, most of all, their antioxidant qualities, tested in the scavenging of ABTS radical, resulted superior to commercially available products.[56] Building on promising preliminary data, we aimed to study here the impact of the ligand

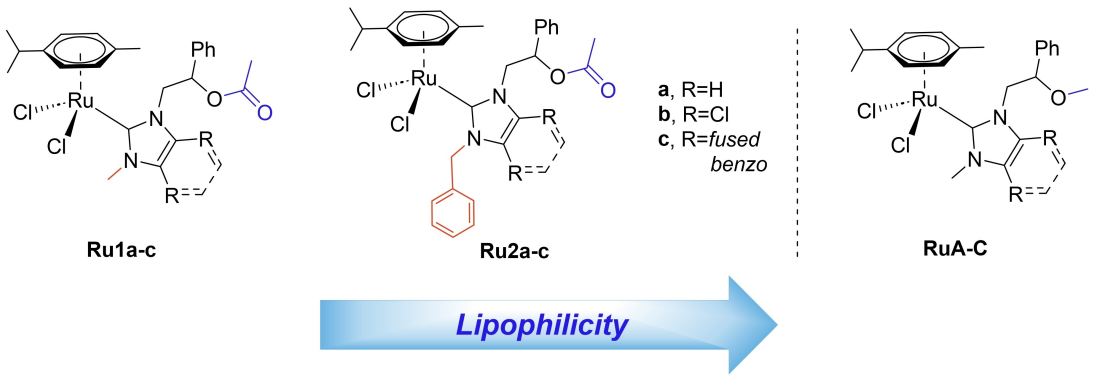

Figure 2. Left to right: Reported RANHC endowed with an ether substituent (**A**–**C**) and novel acetyl substituted complexes **Ru1a**–**c** and **Ru2a**–**c**.

Research Article
doi.org/10.1002/ejic.202400402

amphiphilicity and the counterion on the overall bioactivity, thus we designed a novel family of compounds bearing an ester moiety rather than an alkoxide (Figure 2, **Ru1a**–**c**). Moreover, further evaluations were made by switching the methyl nitrogen substituent with a benzyl unit, in order to increase the lipophilicity and steric hindrance of the metal bonded to the carbenic carbon (Figure 2, **Ru2a**–**c**). Secondly, given the outstanding catalytic performances of Ru^{II} complexes in olefin metathesis,[13,16].we tested all of the synthesized compounds so far in the norbornene ROMP, a benchmark reaction for newly Ru^{II} potential catalysts.

Results and Discussion

Chemistry and Norbornene Polymerization

Synthesis of acetyl endowed proligands **P1a**–**c** and **P2a**–**c** was conveniently performed starting with known intermediates **Ia**–**c**,[57,58] which were subjected to acylation with acetic anhydride to yield **AIa**–**c**.[59] Alkylation with either iodomethane or benzyl bromide led to the respective triplet of congener imidazolium salts (Scheme 1A)).

Synthesis of the Ru^{II} complexes was accomplished following the transmetallation route.[60–62] The appropriate carbene precursor was reacted with silver oxide to yield the respective Ag^{I} complexes; then, metathesis of the latter with commercially available $[(p\text{-cymene})RuCl_2]_2$ gave the desired Ru^{II} complexes, isolated as orange-brownish solids (Scheme 1B)). For all of the novel synthesized complexes, the NMR spectra show the disappearance of the proton on the carbocationic carbon and the notable shift towards the lower field of the NCN carbon, thus confirming the formation of carbene carbon and the desired Ru^{II} adduct, which was further validated by mass spectra.

Since lipophilicity is known to substantially affect bioproperties, logP measurements[63,64] were conducted in order to determine the amphiphilic properties of model complexes **RuB** and **Ru1b**, which solely differ for the ether/ester switch on the wingtip substituent. 1-Octanol/water partition coefficient resulted, respectively, 0.73 and −0.11, indicating a strongly pronounced lipophilicity for acetyl derivatives (see Supporting Information).

Catalytic performances of novel synthesized complexes were assessed in the benchmark ROMP reaction of norbornene, with a 3 μM catalyst loading, and a high (3000:1) monomer/catalyst ratio.[65–68]

According to reported studies, transient Ru-alkylidene active species can be generated *in situ* by either addition in the reaction medium of alkynes,[44,45] cyclopropenes,[46,47] or diazocompounds.[47,48]

Among these, inexpensive ethyl diazoacetate (EDA) was shown to be a productive initiator both in benchmark cross metathesis and ring-opening metathesis.

Basing on these assumptions, novel Ru complexes were investigated in the catalysis both with and without ethyl diazoacetate as the initiator to gain a deeper understanding of the reaction pathway.

Catalysis tests, performed in the optimal conditions individuated by Mauduit and colleagues,[47] are reported in Table 1. All of the novel synthesized pre-catalysts showed good to excellent activity, as indicated by the high conversions to polynorbor-

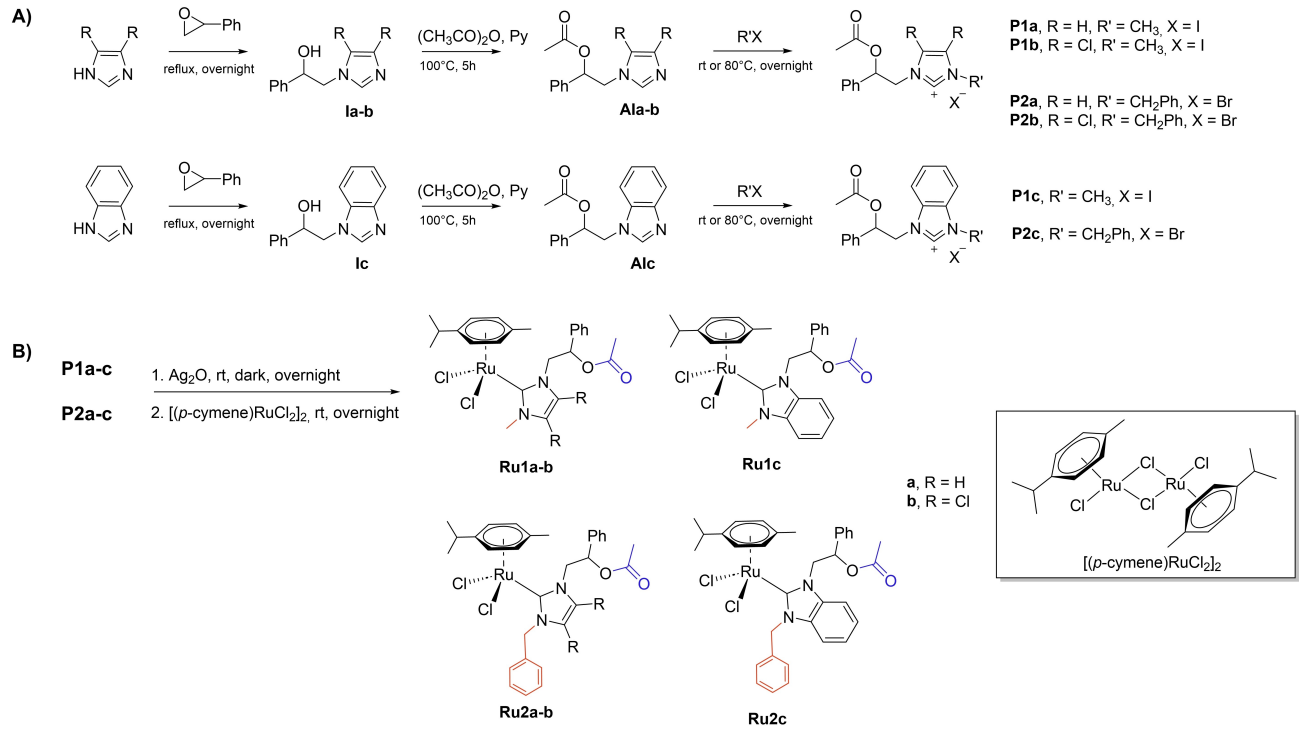

Scheme 1. A) Synthesis of proligands **P1a**–**c**, **P2a**–**c** and B) Ru^{II} complexes **Ru1a**–**c**, **Ru2a**–**c**.

Research Article
doi.org/10.1002/ejic.202400402

Table 1. Norbornene ROMP catalysed by complexes **Ru1a–c**, **Ru2a–c**.

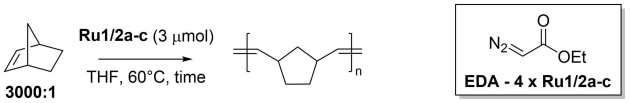

Run[a]	Catalyst (+initiator)	Time (min)	Conversion (%)[b]	*E*/*Z* ratio (%)[c]	Mn (kg/mol)[d]	PDI[d]
1	**Ru1a**	60	Traces	34/66	55.3	9.6
2	**Ru1a** + EDA	60	87	38/62	121.0	5.2
3	**Ru1b**	60	Traces	34/66	18.0	6.9
4	**Ru1b** + EDA	7[e]	99	46/54	44.1	5.6
5	**Ru1c**	60	Traces	24/76	27.8	6.8
6	**Ru1c** + EDA	60[e]	96	44/56	196.1	2.8
7	**Ru2a**	60	n.d.	–	–	–
8	**Ru2a** + EDA	60	91	47/53	71.5	4.0
9	**Ru2b**	60	6	25/75	41.8	3.4
10	**Ru2b** + EDA	7[e]	99	66/34	267.3	4.2
11	**Ru2c**	60	Traces	24/76	182.0	5.1
12	**Ru2c** + EDA	10[e]	97	38/62	155.7	4.5
13	**RuB**	6[e]	95	18/81	12.2	31.0
14	**RuB** + EDA	15[e]	97	16/84	16.7	18.0
15	[(*p*-cymene)$RuCl_2$]$_2$	12[e]	99	34/66	3.3	36.5
16	[(*p*-cymene)$RuCl_2$]$_2$ + EDA	1[e]	99	15/85	3.1	14.4

[a] Reaction conditions: [Ru] 3 μmol, precatalyst:monomer ratio 3000:1, 60 °C, dry THF (5 mL). [b] Conversions determined by ^{1}H NMR ($CDCl_3$), using 2-bromomesytilene as internal standard. [c] Determined by ^{1}H NMR ($CDCl_3$), δ = 5.36 ppm *E* CH=CH, 5.22 ppm, *Z* CH=CH. [d] Determined by GPC (THF). [e] Gelification of the polymer observed.

nene, and elevated M_n, paired with quite narrow PDI_s (polydispersity index), in the presence of EDA as initiator.

Necessary thermal pre-dissociation of the *p*-cymene moiety, in order to generate the 14-electron complex **B**, was performed by 15 minutes treatment of **Ru1a–c**, **Ru2a–c** in dry THF at 60 °C. This allowed the exchange with a labile THF coordinated molecule, then replaced by the formation of the active Ru-alkylidene catalyst **C**, with concomitant nitrogen evolution from ethyl diazoacetate activator. In the presence of the substrate such species gives the conversions to polynorbornene, in the indicated times, in Table 1 (Scheme 2).

Crucial stabilization of the thermally generated 14-electron species **B** (Scheme 2) has been reported as the rate-determining step towards the formation of the catalytically active species.[29,42,47,69]

The beneficial effect of the NHC ligand can be ascertained comparing novel acetyl derivatives **Ru1/2 a–c** with reported ether complexes **RuA–C**.[56] All the novel complexes conversions range from 87% to completion, while alkoxy derivatives lack efficient catalytic activity even in the presence of EDA (Table 1, entries 13–14), as stated by low molecular masses, coupled with broad polydispersity indexes. This may be due to the carbonyl-assisted stabilization of intermediate **B** by means of the acyl group (panel A, Figure 3); the same effect would not be as efficient in the presence of a methoxy group from NHC ligands

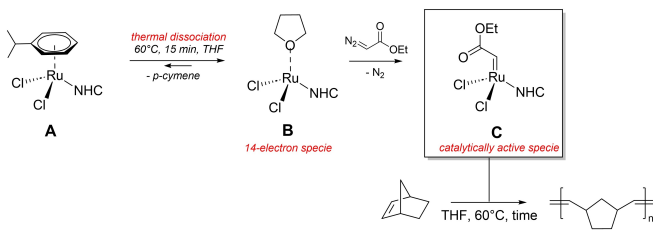

Scheme 2. Mechanism of activation with ethyl diazoacetate. A. Precatalyst Ru1/2a-c is subjected to thermal *p*-cymene dissociation to intermediate B, coordinated by THF. Reaction with EDA yields C, which starts the catalytic cycle.

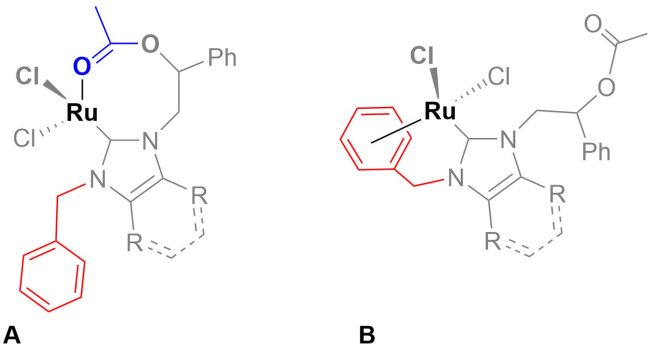

Figure 3. Hypothesized **A**. 14-electron Ru^{II} stabilization assisted by acetyl group; **B**. 14-electron Ru^{II} stabilization assisted by benzyl group.

in **RuA**–**C**. As previously mentioned, the presence of an hemilabile group on the *N*-heterocyclic carbene wingtip, such as the carboxyl residue, can enhance the stability of the catalytically active species, promoting its formation.

Interestingly, no relevant effect was observed switching the backbone NHC substituent from an electron-withdrawing (chloride, **Ru1/2b**) to an electron-donating (fused benzene, **Ru1/2c**), suggesting indeed the need for a steric encumbrance. In fact, both substituents provoke an increase of conversions and M_n, when compared with unsubstituted **Ru1/2a** (entry 2 vs. 4 and 6, and 8 vs. 10 and 12).

Further increase of lipophilicity, gained by substitution of methyl group on one of the nitrogen imidazole heteroatoms in complexes **Ru2a**–**c**, did not lead to conspicuous differences in catalytic performances (entries 7–12). Contrary to what was possible to hypothesize, the benzyl group did not significantly compete with the acetyl carbonyl in the stabilization of the 14-electron Ru^{II} specie (panel B, Figure 3). In fact, the yields are practically the same and the polydipersity indices are only slightly narrower. This behavior could be attributed to the over-stabilization of the complex, in the presence of the phenyl ring, which could donate up to six additional electrons to the metallic centre.

All of the neosynthesized complexes showed superior performances when compared with commercially available [(*p*-cymene)$RuCl_2]_2$. The latter, in fact, in the presence of EDA gave complete conversion, but with high polydispersity (14.4) and reduced M_n (3.1 kg/mol), suggesting, as previously reported in the literature,[43,69] multiple-site polymerization mechanisms and secondary metathesis reactions, including inter- and intra-molecular chain transfer.

As far as stereoselectivity is concerned, no significant *E/Z* ratios were observed, displaying a slight preference for the *Z* product, not exceeding 70%.

Bioactivity

Anticancer Activity

The six new Ru-NHC complexes were evaluated for their anticancer potential against two different breast cancer cell lines, namely the ER-positive MCF-7 and the triple negative MDA MB-231 cells, by the means of MTT assay. The obtained outcomes were expressed as IC_{50} values, calculated after 72 hours of exposure to the studied complexes, which are reported in Table 1. As reference molecule, a well-known anticancer complex, *i.e. Cis*platin, was used. A significant anticancer activity was recorded only for two complexes, **Ru2b** and **Ru2c**, toward both the breast cancer cells, but with a higher activity against the MDA-MB-231 cells, respectively of about four- and three-fold superior with respect to MCF-7 cells. Indeed, **Ru2b** IC_{50} values were of 10.1 ± 0.3 and 45.1 ± 0.06 μM, whereas **Ru2c** values were of 14.7 ± 0.02 and 45.8 ± 0.07 μM, for MDA-MB-231 and MCF-7 cells, respectively. It should be noted that both the active complexes differ for the type and nature of the substituents of the carbene ring. Particularly, **Ru2b** bears two chlorine atoms at the carbene ring, whereas **Ru2c** carbene ring is fused with a benzene scaffold. The other complexes did not show any anticancer activity against both the adopted breast cancer cell lines, at least until the concentration of 50 μM and under the adopted experimental conditions. It can be deduced that the lack of the bulkier benzyl group at the carbenic nitrogen in position 5 (**Ru1a**, **Ru1b** and **Ru1c**) led to the completely drop of the anticancer activity. Furthermore, **Ru2a** possesses the benzyl substituent at N3, but does not have the chlorine atoms at C4 and C5 (**Ru2b**) or the benzene fused to the carbenic ring (**Ru2c**) and is inactive, as well. Finally, **Ru2b** and **Ru2c** impacted MDA-MB-231 cells viability three- and two-fold better than *Cis*platin, respectively. Moreover, proligands **P1a**–**c** and **P2a**–**c**, together with [(*p*-cymene)$RuCl_2]_2$, were tested against both the adopted cell lines, but no effects were evidenced, at least until the concentration of 50 μM.

Antioxidant Activity

The antioxidant effect of the synthesized Ru-NHC complexes was assessed by using the 2,2-diphenyl-1-picrylhydrazyl (DPPH) and the 2,20-azino-bis(3-ethylbenzo-thiazoline-6-sulphonic acid) (ABTS) radicals scavenging assays.

The DPPH scavenging activity of all the Ru-NHC complexes resulted higher compared to the Trolox, used as standard antioxidant in our assay. Indeed, they exhibited a stronger electron donating power, showing IC_{50} values very close to each other, ranging from 1.2 to 2.3 μM (see Table 3). In particular, the best scavenging activity against DPPH radical was recorded by **Ru1b** and **Ru2b**, bearing two chlorine atoms at the carbene ring (IC_{50} values of 1.2 ± 0.1 and 1.3 ± 0.09 μM, respectively), and also by **Ru1c** and **Ru2c** with the carbene ring fused with a benzene scaffold (IC_{50} values of 1.6 ± 0.1 and 1.2 ± 0.1 μM, respectively). Instead, the lack of the two chlorine atoms or the fused benzene ring at the carbene produced a slight reduction of about 2 times in DPPH scavenging activity, as in **Ru1a** and **Ru2a**, which showed IC_{50} values of 2.3 ± 0.09 and 2.1 ± 0.1 μM, respectively. As visible from Table 2, Trolox produced a scavenging activity towards the DPPH radical approximately 17 times lower than the more active complexes, with an IC_{50} value of 20.8 ± 0.04 μM.

To further investigate the Ru-NHC complexes antiradical potential, we measured their ability to interfere with the ABTS radical cation. The outcomes in terms of IC_{50} values of Ru-NHC complexes, alongside the standard Trolox, on ABTS radical are reported in Table 3.

Likewise, in this case, all the Ru-NHC complexes exhibited a higher ABTS scavenging activity than Trolox, which showed an IC_{50} value of 18.3 ± 0.02 μM. All the complexes had a very good antioxidant ability, with IC_{50} values ranging from 39 ± 0.07 nM (**Ru2a**) to 71 ± 0.08 nM (**Ru1a**) (see Table 3). Particularly, the ABTS scavenging activity pattern of the Ru-NHC complexes can be ranked in the following order: **Ru2a** > **Ru1b** > **Ru1c** > **Ru2c** > **Ru2b** > **Ru1a**. Anyway, the scavenging activity of the most active complexes against the ABTS radical cation is about 470 times higher than that measured for Trolox.

Research Article
doi.org/10.1002/ejic.202400402

Table 2. Anticancer activity of the studied Ru-NHC complexes (**Ru1a–c**, **Ru2a–c**), [(*p*-cymene)$RuCl_2]_2$ and *Cis*platin used as reference, expressed as IC_{50} values ± S.E. μM, against two breast cancer cell lines.

IC_{50} ± S.E.		
Compounds	MDA-MB-231	MCF-7
Ru1a	> 50	> 50
Ru2a	> 50	> 50
Ru1b	> 50	> 50
Ru2b	10.1 ± 0.3	45.1 ± 0.06
Ru1c	> 50	> 50
Ru2c	14.7 ± 0.02	45.8 ± 0.07
[(*p*-cymene)$RuCl_2]_2$	> 50	> 50
*Cis*platin	33.8 ± 0.05	24.9 ± 0.05

Proligands (**P1a–c** and **P2a–c**) tested against MDA-MB-231 and MCF-7 showed IC_{50} > 50 μM.

Table 3. Radical scavenging ability against DPPH and ABTS radicals, expressed as IC_{50} ± SE μM, of Ru-NHC complexes (**Ru1a–c**, **Ru2a–c**), [(*p*-cymene)$RuCl_2]_2$ and standard drug (Trolox).

IC_{50} (μM) ± S.E.		
Compounds	DPPH	ABTS
Ru1a	2.3 ± 0.09	7.1×10^{-2} ± 0.08
Ru2a	2.1 ± 0.1	3.9×10^{-2} ± 0.07
Ru1b	1.2 ± 0.1	4.3×10^{-2} ± 0.1
Ru2b	1.3 ± 0.09	6.5×10^{-2} ± 0.04
Ru1c	1.6 ± 0.1	4.5×10^{-2} ± 0.06
Ru2c	1.2 ± 0.1	5.9×10^{-2} ± 0.06
[(*p*-cymene)$RuCl_2]_2$	> 30	0.8 ± 0.07
Trolox	20.8 ± 0.04	18.3 ± 0.02

Proligands (**P1a–c** and **P2a–c**) tested against DPPH and ABTS showed IC_{50} > 30 μM.

The obtained results allowed to conclude that the tested complexes exhibited a higher ability in inhibiting the $ABTS^{\bullet+}$ than DPPH, showing a better antioxidant activity than the well-known antioxidant Trolox. Additionally, proligands **P1a–c** and **P2a–c**, together with [(*p*-cymene)$RuCl_2]_2$, were tested for their antioxidant power against DPPH and ABTS radicals. Proligands were found inactive toward both the radicals, at least until the concentration of 30 μM, whereas the [(*p*-cymene)$RuCl_2]_2$ exhibited an IC_{50} value of 0.8 ± 0.07 against the ABTS radical, but was inactive toward DPPH.

Conclusions

In the plethora of Ru^{II} complexes reported in the past thirty years, very few examples of bio- and catalytically active organometallics are reported. While catalytic activity is broad and related to a number of olefin metathesis reactions and polymerizations, broad-spectrum bioactivity is not as often investigated on the same complexes. In this work, six Ru^{II}-arene-NHC complexes were reported, characterized by increasing lipophilicity granted by acyl and benzyl moieties. Their catalytic activity was assessed in the benchmark norbornene ROMP polymerization, and compared with known, akin complexes and commercial [(*p*-cymene)$RuCl_2]_2$, discovering a remarkable activity and interesting of M_n and polydispersities. Notably, the same complexes resulted discrete as anticancer, while outstanding antioxidant properties were found, with radical scavenging ability against DPPH and ABTS radicals in the low μM and nM order, up to 470 times higher than the one that measured for commercial antioxidant Trolox. The Ru^{II}-arene pharmacophore's flexibility allows for further study of NHC-Ru^{II}-arene complexes. Further derivatization of the arene moiety, substitution with different chelating groups, and diversity of the NHC motif could lead to the development of new metal-based anticancer medicines, which, at the same time, could work as useful catalysts in classical double bonds functionalization.

Experimental Section

Materials and Methods

All reagents were purchased from Merck Italy (Milan, Italy) and TCI Chemicals (Zwijndrecht, Belgium) and used without any purifications. All solvents were bought by Carlo Erba Reagents srl (Milano, Italy) and were distilled over appropriate drying agents under nitrogen before use. The synthesis of Ru-complexes was carried out under a nitrogen atmosphere by using Schlenk techniques in the dark. The glassware used was dried in an oven at 120 °C overnight. Organic molecules were purified by flash column chromatography using silica gel 60 (230–400 mesh) purchased from Merck Italy. Thin layer chromatography (TLC) was performed using silica gel 60 aluminum foils with F254 fluorescent indicator. Deuterated solvents were dried on molecular sieves. ^1H and ^{13}C nuclear magnetic resonance spectra (NMR) were acquired on a Bruker Avance 300 spectrometer (300 MHz for ^1H; 75 MHz for ^{13}C), a Bruker AVANCE 400 spectrometer (400 MHz for ^1H; 100 MHz for ^{13}C) and a Bruker AVANCE 600 spectrometer (600.13 MHz for ^1H, 150.90 MHz for ^{13}C), operating at 298 K. NMR samples were prepared by dissolving about 15 mg of the compound in 0.5 mL of deuterated solvent (Eurisotop Cambridge Isotope Laboratories, Cambridge, UK). The chemical shifts of ^1H-NMR and ^{13}C-NMR spectra are referenced using the residual proton impurities of the deuterated solvents. ^1H-NMR were reported relative to DMSO-d_6 δ 2.50 ppm, $CDCl_3$ δ 7.26 ppm, THF-d_8 δ 3.58 ppm and CD_3CN δ 1.72 ppm and δ 1.94 ppm. ^{13}C-NMR were reported relative to DMSO-d_6 δ 39.52 ppm, $CDCl_3$ δ 77.16 ppm, THF-d_8 δ 67.21 ppm and δ 25.31 ppm, and CD_3CN δ 1.32 ppm δ 118.26 ppm. The spectra multiplicities are indicated as follows: singlet (s), doublet (d), triplet (t), multiplet (m), broad (br). MALDI-MS mass spectra were obtained by Bruker SolariX XR Fourier transform ion cyclotron resonance mass spectrometer (Bruker Daltonik GmbH, Bremen, Germany) with a 7 T refrigerated actively shielded superconducting magnet (Bruker Biospin, Wissembourg, France). MALDI ion source (Bruker Daltonik GmbH, Bremen, Germany) was used the samples in positive ion mode. The mass range was set to m/z 200–3000. The laser power was 28% and 22 laser shots were utilized for each scan. The mass spectra were calibrated externally using a mix of peptide clusters in MALDI ionization positive ion mode. ESI-MS spectra were achieved using a Waters Quattro Micro triple-quadrupole mass spectrometer equipped with an electrospray ionization source. GPC measurements were performed on a Waters 1525 binary equipped with a

Research Article
doi.org/10.1002/ejic.202400402

Waters 2414 RI detector using four Styragel columns (range 1000–1,000,000 Å) (Waters Corporation, Milford, Massachusetts, United States). Ultraviolet-visible (UV-Vis) measurements were performed with an Agilent Varian Cary 50 spectrophotometer (Agilent Technologies Inc., Santa Clara, California, USA).

Synthesis of the Imidazolium Salts, Proligands P1a–c, P2a–c

Ia–c were synthesized following the procedure reported in literature.[58]

Synthesis of AIa–c

AIa–c were synthesized using a procedure reported in the literature, modified for our purposes.[70] **Ia–c** (1.00 eq) and pyridine (3.00 eq) are placed in a two-necked flask equipped with a magnetic stirrer and a condenser, under a nitrogen atmosphere. After dissolving **Ia–c**, acetic anhydride (5.00 eq) was added. The reaction mixture was heated at 100 °C for 5 hours. The solution was diluted with 30 mL of diethyl ether and extracted with water (3×30 mL). The organic phase was dried with $MgSO_4$, and filtered. The solvent was removed under reduced pressure. The product was obtained as a greenish oil. Yields: **AIa** 89 %, **AIb** 78 %, **AIc** 61 %.

2-(1H-imidazol-1-yl)-1-phenylethyl acetate (AIa)

^{1}H-NMR (ppm, CD_3CN, 300 MHz) δ: 7.53 (1H, s, NC***H***N), 7.33–7.30 (5H, overlapping signals, Ar-***H***), 7.01 and 6.94 (2H, s, NC***H***=C***H***N), 5.95 (1H, t, *J* = *5.89 Hz*, $NCH_2C\boldsymbol{H}$), 4.33 (2H, d, *J* = *5.89 Hz*, $NC\boldsymbol{H_2}CH$), 2.01 (3H, s, $COC\boldsymbol{H_3}$).

^{13}C-NMR (ppm, CD_3CN, 75 MHz) δ: 170.62 (***C***=O), 138.80 (*ipso carbon of aromatic ring*), 138.41 (N***C***HN), 129.61 (×2), 129.47, 129.04 (×2), 127.26, 121.05 (*Ph-group* and N***C***H***C***HN), 75.34 ($NCH_2\boldsymbol{C}H$), 52.02 (NCH_2), 21.11 ($CO\boldsymbol{C}H_3$).

MALDI-MS (CH_3CN) calcd/found (m/z): $[C_{13}H_{14}N_2O_2]^+$ 231.1128/231.1129.

2-(4,5-dichloro-1H-imidazol-1-yl)-1-phenylethyl acetate (AIb)

^{1}H-NMR (ppm, DMSO-d_6, 300 MHz) δ: 7.72 (1H, s, NC***H***N), 7.40–7.32 (5H, overlapping signals, Ar-***H***), 6.00 (1H, t, *J* = *5.86 Hz*, $NCH_2C\boldsymbol{H}$), 4.40 (2H, m, *J* = *5.86 Hz*, $NC\boldsymbol{H_2}CH$), 2.05 (3H, s, $COC\boldsymbol{H_3}$).

^{13}C-NMR (ppm, DMSO-d_6, 100 MHz): δ 169.25 (***C***=O), 136.70 (*ipso carbon of aromatic ring*), 136.39 (N***C***HN), 128.63 (×2), 126.28 (×2), 124.09 (*Ph-group* and N***C***Cl***C***ClN), 72.89 ($NCH_2\boldsymbol{C}H$), 49.56 ($N\boldsymbol{C}H_2$), 20.56 ($CO\boldsymbol{C}H_3$).

MALDI-MS (CH_3CN) calcd/found (m/z): $[C_{13}H_{12}Cl_2N_2O_2]^+$ 299.0349/299.0351.

2-(1H-benzoimidazol-1-yl)-1-phenylethyl acetate (AIc)

^{1}H-NMR (ppm, DMSO-d_6, 600 MHz) δ: 8.09 (1H, s, NC***H***N), 7.65–7.63 (2H, overlapping signals, Ar-***H***), 7.40–7.37 (5H, overlapping signals, Ar–***H***), 7.25 (1H, t, J_{ortho} = *7.29 Hz*, Ar-***H***), 7.19 (1H, t, J_{ortho} = *7.29 Hz*, Ar–***H***), 6.07 (1H, t, *J* = *6.08 Hz*, $NH_2C\boldsymbol{H}$), 4.67 (2H, m, $NC\boldsymbol{H_2}CH$), 1.92 (3H, s, $COC\boldsymbol{H_3}$).

^{13}C-NMR (ppm, DMSO-d_6, 150 MHz) δ: 169.26 (***C***=O), 144.37 (N***C***HN), 143.06, 137.21, 134.04, 128.52, 128.41 (×2), 126.46 (×2), 122.30, 121.48, 119.34, 110.65 (*Ph-groups*), 73.66 ($NCH_2\boldsymbol{C}H$), 48.49 ($N\boldsymbol{C}H_2$), 20.59 ($CO\boldsymbol{C}H_3$).

MALDI-MS (CH_3CN) calcd/found (m/z): $[C_{17}H_{16}N_2O_2]^+$ 281.1284/281.1288.

Synthesis of P1a–c

To a solution of **AIa–c** (1.00 eq) in acetonitrile (0.5 M) was added methyl iodide (7.00 eq) and the resultant solution was stirred at room temperature for 18 h. After the solvent was removed under reduced pressure, the residual powder was washed with acetone (3×10 mL) and dried by reduced pressure to obtain the product (**P1a–c**) as a white powder. Yields: **P1a** 85 %, **P1b** 66 %, **P1c** 52 %.

N-Methyl, N′-(2-acethoxy-2-phenyl)ethyl imidazolium iodide (P1a)

^{1}H-NMR (ppm, CD_3CN, 400 MHz) δ: 8.76 (1H, s, NC***H***N), 7.41–7.35 (7H, overlapping signals, Ar-***H*** and NC***H***=C***H***N,), 6.01 (1H, m, $NCH_2C\boldsymbol{H}$), 4.56 (2H, m, $NC\boldsymbol{H_2}CH$), 3.83 (3H, s, $NC\boldsymbol{H_3}$), 2.05 (3H, s, $COC\boldsymbol{H_3}$).

^{13}C-NMR (ppm, CD_3CN, 100 MHz) δ: 170.49 (***C***=O), 137.70 (*ipso carbon of aromatic ring*), 137.15 (N***C***HN), 129.88, 129.81, 127.22 (×2), 124.40, 124.21 (*Ph-group*), 74.12 ($NCH_2\boldsymbol{C}H$), 54.23 ($N\boldsymbol{C}H_2$), 37.08 ($N\boldsymbol{C}H_3$), 21.15 ($CO\boldsymbol{C}H_3$).

MALDI-MS (CH_3CN) calcd/found (m/z): $[C_{14}H_{16}N_2O_2]^+$ 245.1284/245.1282.

N-Methyl, N′-(2-acethoxy-2-phenyl)ethyl-4,5-dichloro-imidazolium iodide (P1b)

^{1}H-NMR (ppm, DMSO-d_6, 400 MHz) δ: 9.43 (1H, s, NC***H***N), 7.43–7.39 (5H, overlapping, Ar–***H***), 5.98 (1H, m, $NCH_2C\boldsymbol{H}$), 4.69 (2H, m, $NC\boldsymbol{H_2}CH$), 3.87 (3H, s, $NC\boldsymbol{H_3}$), 2.08 (3H, s, $COC\boldsymbol{H_3}$).

^{13}C-NMR (ppm, DMSO-d_6, 75 MHz) δ: 169.39 (***C***=O), 137.21 (N***C***HN), 135.77 (*ipso carbon of aromatic ring*), 128.98, 128.85, 126.33 (×2), 119.43, 118.87 (*Ph-group* and N***C***Cl***C***ClN), 72.46 ($NCH_2\boldsymbol{C}H$), 51.63 ($N\boldsymbol{C}H_2$), 35.23 ($N\boldsymbol{C}H_3$), 20.81 ($CO\boldsymbol{C}H_3$).

MALDI-MS (CH_3CN) calcd/found (m/z): $[C_{14}H_{15}Cl_2N_2O_2]^+$ 313.0505/313.0506.

N-Methyl, N′-(2-acethoxy-2-phenyl)ethyl-benzoimidazolium iodide (P1c)

^{1}H-NMR (ppm, DMSO-d_6, 300 MHz) δ: 9.73 (1H, s, NC***H***N), 8.07–8.00 (2H, overlapping signals, Ar-***H***), 7.70–7.67 (2H, overlapping signals, Ar-***H***), 7.49–7.38 (5H, overlapping signals, Ar–***H***), 6.13 (1H, m, $NCH_2C\boldsymbol{H}$), 4.99 (2H, m, $NC\boldsymbol{H_2}CH$), 4.12 (3H, s, $NC\boldsymbol{H_3}$), 2.07 (3H, s, $COC\boldsymbol{H_3}$).

^{13}C-NMR (ppm, DMSO-d_6, 75 MHz): δ 169.43 (***C***=O), 143.24 (N***C***HN), 136.29, 131.50, 131.36, 128.76, 126.51, 113.82, 113.53 (*Ph-groups*), 73.20 ($NCH_2\boldsymbol{C}H$), 50.42 ($N\boldsymbol{C}H_2$), 33.47 ($N\boldsymbol{C}H_3$), 20.69 ($CO\boldsymbol{C}H_3$).

MALDI-MS (CH_3CN) calcd/found (m/z): $[C_{18}H_{18}N_2O_2]^+$ 295.1441/295.1448.

Synthesis of P2a–c

AIa–c (1.00 eq) in acetonitrile (0.5 M) were introduced into a two-necked flask, equipped with a magnetic stirrer and condenser. Subsequently, benzyl bromide (1.50 eq) was added and the reaction mixture was stirred overnight at 80 °C in a nitrogen atmosphere. After the solvent was removed under reduced pressure. The residue

Research Article
doi.org/10.1002/ejic.202400402

obtained was purified by column chromatography on silica gel using eluent hexane: ethyl acetate (9:1) to obtain the product as a white solid. Yields: **P2a** 66%, **P2b** 88%, **P2c** 34%.

N-Benzyl, N′-(2-acethoxy-2-phenyl)ethyl-imidazolium bromide (P2a)

^{1}H-NMR (ppm, CD_3CN, 400 MHz) δ: 9.31 (1H, s, NC***H***N), 7.50–7.32 (12H overlapping signals, Ar-***H*** and NC***H***=C***H***N), 6.06 (1H, m, NCH_2***CH***), 5.45 (2H, s, NC***H***$_2$Ph), 4.59 (2H, m, NC***H***$_2$CH), 2.02 (3H, s, COC***H***$_3$).

^{13}C-NMR (ppm, CD_3CN, 62.5 MHz) δ: 170.43 (***C***=O), 137.61 (N***C***HN), 137.00, 135.04 (*ipso carbon of aromatic rings*), 130.03 (×2), 129.95, 129.67 (×3), 129.44, 129.25, 127.05 (×2), 124.53, 123.00 (*Ph-groups* and N***C***H***C***HN), 73.91 (NCH_2***C***H), 54.19 (N***C***H$_2$Ph), 53.40 (N***C***H$_2$CH), 21.11 (CO***C***H$_3$).

MALDI-MS (CH_3CN) calcd/found (m/z): $[C_{20}H_{21}N_2O_2]^+$ 321.1597/321.1615.

N-Benzyl, N′-(2-acethoxy-2-phenyl)ethyl-4,5-dichloro-imidazolium bromide (P2b)

^{1}H-NMR (ppm, $CDCl_3$, 600 MHz) δ: 11.27 (1H, s, NC***H***N), 7.46–7.35 (10H, overlapping, Ar-***H***), 6.12 (1H, m, NCH_2***CH***), 5.63 (1H, d, *J*=*18.0 Hz*, NC***H***HPh), 5.59 (1H, d, *J*=*18.0 Hz*, NCH***H***Ph), 4.92 (1H, dd, NC***H***HCH, J_{gem}=*5.84 Hz*, $J_{vicinal}$=*4.70 Hz*), 4.76 (1H, dd, NCH***H***CH, J_{gem}=*5.84 Hz*, $J_{vicinal}$=*14.70 Hz*), 2.08 (3H, s, COC***H***$_3$).

^{13}C-NMR (ppm, $CDCl_3$, 150 MHz): δ 170.68 (***C***=O), 139.18 (N***C***HN), 135.00 and 132.35 (*ipso carbon of aromatic rings*), 130.51, 130.36, 130.28, 130.02, 129.76 (×2), 129.51 (×2) and 127.25 (×2) (*Ph-groups)*, 120.31 and 119.82 (N***C***Cl***C***ClN), 73.12 (NCH_2***C***H), 53.40 (N***C***H$_2$CH), 53.18 (N***C***H$_2$Ph), 21.76 (CO***C***H$_3$).

MALDI-MS (CH_3CN) calcd/found (m/z): $[C_{20}H_{19}Cl_2N_2O_2]^+$ 389.0818/389.0818.

N-Benzyl, N′-(2-acethoxy-2-phenyl)ethyl-4,5-benzoimidazolium bromide (P2c)

^{1}H-NMR (ppm, DMSO-d_6, 300 MHz) δ: 9.85 (1H, s, NC***H***N), 8.12 (1H, d, J_{ortho}=*7.81 Hz*, Ar-***H***), 7.96 (1H, d, J_{ortho}=*7.81 Hz*, Ar-***H***), 7.66 (2H, m, Ar-***H***), 7.43–7.38 (10H, overlapping signals, Ar-***H***), 6.21 (1H, m, NCH_2***CH***), 5.79 (2H, br s, NC***H***$_2$Ph), 5.02 (2H, br s, NC***H***$_2$CH), 1.95 (3H, s, COC***H***$_3$).

^{13}C-NMR (ppm, DMSO-d_6, 75 MHz) δ: 169.28 (***C***=O), 142.99 (N***C***HN), 136.15, 133.86, 131.64, 130.52, 129.06 (×2), 128.82 (×2), 128.73 (×2), 128.19 (×2), 126.79 (×2), 126.43 (×2), 114.24, 113.81 (*Ph-groups)*, 72.82 (NCH_2***C***H), 50.55 (N***C***H$_2$CH), 49.88 (N***C***H$_2$Ph), 20.64 (CO***C***H$_3$).

MALDI-MS (CH_3CN) calcd/found (m/z): $[C_{24}H_{23}N_2O_2]^+$ 371.1754/371.1765.

Synthesis of Ru1a–c and Ru2a–c Complexes

Ruthenium complexes **Ru1a**–**c** and **Ru2a**–**c** were synthesized by *trans*-metalation from silver complexes, following the procedure reported in our previous study.[56] The imidazolium salt, **P1a**–**c** or **P2a**–**c** (1.00 eq), and Ag_2O (0.50 eq) were stirred in dichloromethane (0.02 M) in darkness at room temperature overnight. Dichloro(*p*-cymene)ruthenium(II) dimer (0.5 eq) was added, and the mixture was stirred for 12 h at room temperature. After filtration the solvent was removed by reduced vacuum and the brownish-orange powder obtained was washed with hexane (3×10 mL). Yields: **Ru1a** 76%, **Ru1b** 51%, **Ru1c** 94%, **Ru2a** 27%, **Ru2b** 88%, **Ru2c** 91%.

Ru1a

^{1}H-NMR (ppm, $CDCl_3$, 600 MHz) δ: 7.48–7.04 (7H, overlapping signals, Ar-***H*** and NC***H***=C***H***N) 6.13 (1H, br m, NCH_2***CH***), 5.34 (2H, br m, *p-cymene* Ar-***H***), 5.04 (2H, m, NC***H***$_2$CH), 4.80–4.50 (2H, br, *p-cymene* Ar-***H***), 3.96 (3H, s, Ar-C***H***$_3$), 2.86 (1H, m, C***H***$(CH_3)_2$), 2.05 (3H, s, NC***H***$_3$), 1.94 (3H, s, COC***H***$_3$), 1.21–1.19 (6H, overlapping, CH(C***H***$_3)_2$).

^{13}C-NMR (ppm, $CDCl_3$, 150 MHz) δ: 175.30 (***C***=O), 169.55 (N***C***N), 137.75 (*ipso-carbon of aromatic ring*) 128.89, 128.79 (×2), 128.49, 126.75 (×2), 126.47, 124.09, 123.06 (*Ph groups* and N***C***H=***C***HN), 109.28, 98.82, 85.79, 81.93 (*aromatic carbon p-cymene*), 73.54 (NCH_2***C***H), 55.31 (N***C***H_2CH), 39.79 (N***C***H_3), 30.74 (*p*-cymene, ***C***HC_2H_6), 22.30 (CO***C***H_3), 21.24 (*p*-cymene, CH***C***$_2H_6$), 18.62 (*p*-cymene, C***C***H_3).

ESI-MS (CH_2Cl_2) calcd/found (m/z): $[C_{24}H_{30}ClN_2O_2Ru]^+$ 515.1037/515.1054

Ru1b

^{1}H-NMR (ppm, THF-d_8, 300 MHz) δ: 7.57 (2H, d, Ar-***H***), 7.40–7.30 (3H, overlapping signals, Ar-***H***), 6.40 (1H, m, NCH_2***CH***), 5.58 (1H, br s, *p-cymene* Ar-***H***), 5.50 (2H, s, NC***H***$_2$CH), 5.28 (3H, broad, *p-cymene* Ar-***H***), 4.06 (3H, s, Ar-C***H***$_3$), 3.01 (1H, m, C***H***$(CH_3)_2$), 2.01 (3H, s, NC***H***$_3$), 1.99 (3H, s, COC***H***$_3$), 1.30–1.26 (6H, overlapping, CH(C***H***$_3)_2$).

^{13}C-NMR (ppm, THF-d_8, 75 MHz) δ: 179.06 (***C***=O), 168.07 (N***C***N), 137.04 (*ipso-carbon of aromatic ring*), 127.52, 127.26, 125.70, 117.24, 116.69 (*Ph groups* and N***C***Cl=***C***ClN), 109.28, 98.82, 85.79, 81.93 (*aromatic carbon p-cymene*) 73.78 (NCH_2***C***H), 53.18 (N***C***H_2CH), 37.53 (N***C***H_3), 29.70 (*p-cymene*, ***C***$H(C_2H_6)$, 22.43 (CO***C***H_3), 19.14 (*p-cymene*, CH(***C***$_2H_6$), 16.97 (*p-cymene*, C***C***H_3).

ESI-MS (CH_2Cl_2) calcd/found (m/z): $[C_{24}H_{28}Cl_3N_2O_2Ru]^+$ 583.0254/583.0728

Ru1c

^{1}H-NMR (ppm, THF-d_8, 300 MHz) δ: 7.52–7.29 (9H overlapping signals, Ar–***H***), 6.51 (1H, br s, NCH_2***CH***), 5.59–5.42 (3H, overlapping signals, Ar–***H*** *p-cymene*), 5.18 (2H, br s, NC***H***$_2$CH), 4.75 (1H, br s, Ar–***H*** *p-cymene*) 4.27 (3H, s, Ar–C***H***$_3$), 3.06 (1H, m, C***H***$(CH_3)_2$), 2.48 (3H, s, NC***H***$_3$), 2.44 (3H, s, COC***H***$_3$), 1.30 and 1.28 (6H, overlapping signals, CH(C***H***$_3)_2$).

^{13}C-NMR (ppm, THF-d_8, 75 MHz): δ 169.92 (***C***=O), 162.99 (N***C***N), 136.83 (*ipso-carbon of aromatic ring*), 129.87, 129.42, 129.37, 128.99, 128.63, 127.67, 127.28, 126.69, 123.26, 122.86 and 117.15 (aromatic carbons), 110.49, 98.90, 82.07, 79.30, 79.09, 78.87 (*aromatic carbon p-cymene*), 74.27 (NCH_2***C***H), 48.70 (N***C***H_2CH), 37.28 (N***C***H_3), 31.42 (*p-cymene*, ***C***HC_2H_6), 20.09 (CO***C***H_3), 18.46 (*p-cymene*, CH***C***$_2H_6$), 15.48 (*p-cymene*, C***C***H_3).

ESI-MS (CH_2Cl_2) calcd/found (m/z): $[C_{28}H_{32}Cl_2N_2O_2Ru]^+$ 565.1190/565.1210

Ru2a

^{1}H-NMR (ppm, $CDCl_3$, 600 MHz): δ 7.53–7.26 (11H, o, *Ph-groups*,), 6.85 (1H, bs, *Ph-groups*,), 6.21(1H, bs, NCH_2C***H***,), 5.85 (1H, o, *Ph-group of p-cymene*), 5.63 (1H, o, *Ph-group of p-cymene*), 5.37–5.30 (2H, o, NC***H***$_2$CH), 5.01 (2H, bs, NC***H***$_2$Ph), 4.50 (1H, m, *Ph-group of p-cymene*), 2.81 (1H, m, C***H*** *of p-cymene*), 2.08 (3H, s, C***H***$_3$ *of p-cymene*), 1.97 (3H, s, COC***H***$_3$), 1.21 (6H, o, CH(C***H***$_3)_2$ *of p-cymene*).

^{13}C-NMR (ppm, $CDCl_3$, 150 MHz): δ 176.90 (***C***=O), 168.91 (N***C***N), 137.39 (*ipso-carbon of aromatic ring*), 137.39, 129.27, 128.95, 128.80, 128.11, 127.89, 126.98, 123.19, 122.99 (*aromatic carbons*), 108.42, 98.27 (*aromatic carbon p-cymene*), 85.91 (NCH_2***C***H), 85.41, 83.72, 82.25, 81.79 (*aromatic carbon p-cymene*), 55.49 (N***C***H_2Ph), 55.21 (N***C***H_2CH), 30.85 (*p-cymene*, ***C***HC_2H_6), 23.10 (CO***C***H_3), 22.17 and 21.32 (*p-cymene*, CH***C***$_2H_6$), 18.70 (*p-cymene*, C***C***H_3).

ESI-MS (CH_2Cl_2) calcd/found (m/z): $[C_{30}H_{34}ClN_2O_2Ru]^+$ 591.1347/591.1414

Ru2b

^{1}H-NMR (ppm, THF-d_8, 600 MHz) δ: 7.62 (2H, d, *Ph-group*), 7.40 (2H, t, *J*=*8.84 Hz*, Ar–***H***), 7.34 (3H, t, *J*=*7.52 Hz*, Ar–***H***), 7.25 (1H, t, *J*=*7.61 Hz*, Ar–***H***), 7.11 (2H, d, *J*=*7.61 Hz*, Ar–***H***) 6.55 (1H, br s, 2H, Ar–***H***), 5.95 (1H, br s, NCH_2C***H***), 5.51 (3H, overlapping signals, NC***H***$_2$CH and *p-cymene* Ar–***H***), 5.19 (2H, br s NC***H***$_2$Ph), 4.96 (1H, br ss, *p-cymene* Ar-***H***), 2.77 (1H, m, C***H***$(CH_3)_2$), 2.08 (3H, s, Ar-C***H***$_3$), 1.87 (3H, s, COC***H***$_3$), 1.23–1.20 (6H, overlapping signals, CH(C***H***$_3)_2$).

^{13}C-NMR (ppm, THF-d_8, 150 MHz): δ 182.60 (***C***=O), 170.06 (N***C***N), 139.74 (*ipso-carbon of aromatic ring*), 129.24, 129.14, 129.08, 127.78, 127.56, 126.83, 126.78, 119.49, 119.35 (*aromatic carbons* and N***C***Cl***C***ClN), 107.96, 98.08, 87.39, 87.18, 87.01, 84.43 (*aromatic carbons p-cymene*), 74.96 (NCH_2***C***H), 55.43 (N***C***H_2Ph), 54.81 (N***C***H_2CH), 31.39 (*p-cymene*, ***C***HC_2H_6), 22.73 (CO***C***H_3), 22.53 and 20.83 (*p*-cymene, CH***C***$_2H_6$), 18.29 (*p-cymene*, C***C***H_3).

ESI-MS (CH_2Cl_2) calcd/found (m/z): $[C_{30}H_{32}Cl_3N_2O_2Ru]^+$ 695.03315/695.3949.

Ru2c

^{1}H-NMR (ppm, THF-d_8, 300 MHz) δ: 7.91 (1H, br s, Ar–***H***), 7.73 (2H, br s, Ar–***H***), 7.42–7.04 (11H, overlapping signals, Ar–***H***), 6.63 (1H, br s, NCH_2C***H***), 6.31 (1H, d, *J*=*17.20 Hz*, *p-cymene* Ar–***H***), 6.13 (1H, d, *J*=*17.20 Hz*, *p-cymene* Ar–***H***) 5.55–5.43 (2H, overlapping signals, NC***H***$_2$CH), 5.12 (2H, br s, NC***H***$_2$Ph), 4.86 (1H, m, *p-cymene* Ar–***H***), 2.89 (1H, m, C***H***$(CH_3)_2$), 1.73 (3H, s, Ar–C***H***$_3$), 1.70 (3H, s, COC***H***$_3$), 1.23 (6H, overlapping signals, CH(C***H***$_3)_2$).

^{13}C-NMR (ppm, THF-d_8, 75 MHz): δ 194.73 (***C***=O), 176.83 (N***C***N), 139.18 (*ipso-carbon of aromatic ring*), 137.47, 136.39, 129.13, 127.96, 127.71, 123.22, 122.94, (*aromatic carbons*), 112.34, 109.47, 98.93, 89.53, 88.64, 83.77 (*aromatic carbons p-cymene*), 54.55 (N***C***H_2Ph), 54.43 (N***C***H_2CH), 31.63 (*p-cymene*, ***C***HC_2H_6), 23.27 (CO***C***H_3), 22.22 and 20.73 (*p*-cymene, CH***C***$_2H_6$), 18.54 (*p-cymene*, C***C***H_3).

ESI-MS (CH_2Cl_2) calcd/found (m/z): $[C_{34}H_{36}ClN_2O_2Ru]^+$ 641.1509/641.1535.

General Polymerization Procedure

In a general ROMP experiment, 3.0 μmol of catalyst were introduced in 0.15 mL of dry THF, and the solution was stirred for 15 minutes at 60 °C. A second solution was prepared introducing NBE (9.0 mmol) and EDA (12 μmol) into 5 mL of THF. The first solution containing the catalyst was then injected into the second solution. The polymerization was quenched using ethyl vinyl ether and the polymer was coagulated in methanol, filtered and dried under vacuum.

Determination of the Logarithm of the Partition Coefficient (LogP)

The logarithm of the partition coefficient (LogP) was obtained by following the procedure reported in the literature with a slight modification.[63,71] 100 mL of water (distilled after milli-Q purification) and 100 mL of 1-octanol were stirred together for 72 h to allow saturation of both phases. Five standard solutions of complexes were prepared in the 1-octanol phase and other five in the water phase (20, 40, 60, 80 and 100 μM), and a calibration curve (absorbance vs concentration) was obtained using UV/vis spectroscopy. A further solution of both complexes was prepared in a 1-octanol phase (50 μM) and an equal volume of water was added. The biphasic solutions were mixed for 20 minutes and then centrifuged for 1 h at 6500 rpm to allow separation. Concentration in each phase was determined by UV/VIS. LogP was calculated using the following formula log[complex]oct/[complex]H_2O. **RuB**, logP 0.73; **Ru1b**, logP −0.11.

Cell Cultures

The two breast cancer cells used in this assay, the human estrogen receptor positive [(ER(+)] MCF-7 and the triple negative MDA-MB-231 breast cancer cells, were obtained from American Type Culture Collection (ATCC, Manassas, VA, USA) and cultured as already indicated.[72] The cell cultures were maintained at the temperature of 37 °C in a humidified atmosphere containing 5 % CO_2.

MTT Assay

MTT assays [Sigma Aldrich (St. Louis, MO, USA)] were employed to evaluate the *in vitro* anticancer activities of all the studied compounds, as already defined.[73] The compounds were tested at different concentrations (0.1-1-10-25-50 μM) for 72 h. The IC_{50} values were calculated from the percent (%) of control using GraphPad Prism 9 (GraphPad Software, La Jolla, CA, USA).

2,2-Diphenyl-1-Picrylhydrazyl (DPPH) Assay

The radical scavenging properties of the Ru-NHC complexes on the 1,1-diphenyl-2-picrylhydrazil (DPPH) radical were evaluated as previously described.[56]

All the compounds were used at different concentrations (0.1, 1, 10, 20 and 30 μM) and the DPPH radical scavenging activity, measured at 515 nm using a microplate reader, was expressed as inhibition percentages (%I_{DPPH}) compared to the initial concentration of DPPH (control) according to the following expression:

$$I_{DPPH}\ (\%) = [(ABS_{CTRL} - ABS_{sample})/ABS_{CTRL}] * 100$$

where ABS_{CTRL} and ABS_{sample} are the absorbance at 515 nm in the control and in the presence of samples, respectively. The obtained I_{DPPH} percentages allowed us to calculate the IC_{50} values using Graph-Pad Prism 9 software (GraphPad Inc., San Diego, CA, USA). Trolox was employed as a positive control.

2,20-Azinobis(3-ethylbenzothiazoline-6-sulfonic acid (ABTS) Assay

The radical scavenging properties of the complexes on a 2,20-azino-bis(3-ethylbenzothiazoline-6-sulfonate) radical cation ($ABTS^+$) were evaluated as previously described.[56]

All the compounds were used at different concentrations (0.001, 0.01, 0.1, 1, 10, 20 and 30 μM) and the ABTS radical scavenging activity, measured at 730 nm using a microplate reader, was expressed as inhibition percentages (%I_{ABTS}) compared to the control, according to the following expression:

$$I_{ABTS}\ (\%) = [(ABS_{CTRL} - ABS_{sample})/ABS_{CTRL}] * 100$$

where ABS_{CTRL} and ABS_{sample} are the absorbance at 730 nm in the control and in the presence of samples, respectively.

IC_{50} values were calculated from the %I_{ABTS} using GraphPad Prism 9 software (Graph-Pad Inc., San Diego, CA, USA). Trolox was employed as a positive control.

Acknowledgements

Dr. Patrizia Oliva and Dr. Patrizia Iannece are acknowledged for technical assistance. Ms. Deborah Limone is acknowledged for experimental work. We acknowledge financial support under the National Recovery and Resilience Plan (NRRP), Mission 4, Component 2, Investment 1.1, Call for tender No. 104 published on 2.2.2022 by the Italian Ministry of University and Research (MUR), funded by the European Union – NextGenerationEU – Project Title HyMTA (Hybrid Multi-Target Agents) Synthesis and biological evaluation of chimeric hybrid molecules containing NHC-metal complexes and carbazole moieties, as innovative multi-target anticancer and antiviral agents – CUP C53D23004490001- Grant Assignment Decree No. 1064 adopted on 18/07/2023 by the Italian Ministry of Ministry of University and Research (MUR) and call for tender No. 1409 published on 14.9.2022 by the Italian Ministry of University and Research (MUR), funded by the European Union – NextGenerationEU – Project Title Enhanced pharmacological activity of noble metal carbene-N-heterocyclic complexes by oligopeptide counterion – CUP C53D23007800001 – Grant Assignment Decree No. 1384 adopted on 01/09/2023 by the Italian Ministry of Ministry of University and Research (MUR).

Conflict of Interests

The authors declare no conflict of interest.

Data Availability Statement

The data that support the findings of this study are available in the supplementary material of this article.

Keywords: Ruthenium-arene-NHC · ROMP · Norbornene · Antioxidant · Anticancer

[1] D. Bourissou, O. Guerret, F. P. Gabbaï, G. Bertrand, *Chem. Rev.* **2000**, *100*, 39–92.
[2] M. N. Hopkinson, C. Richter, M. Schedler, F. Glorius, *Nature* **2014**, *510*, 485–496.
[3] K.-S. Feichtner, V. H. Gessner, *Chem. Commun.* **2018**, *54*, 6540–6553.
[4] R. F. R. Jazzar, S. A. Macgregor, M. F. Mahon, S. P. Richards, M. K. Whittlesey, *J. Am. Chem. Soc.* **2002**, *124*, 4944–4945.
[5] S. Gaillard, C. S. J. Cazin, S. P. Nolan, *Acc. Chem. Res.* **2012**, *45*, 778–787.
[6] C. M. Crudden, D. P. Allen, *Coord. Chem. Rev.* **2004**, *248*, 2247–2273.
[7] M. J. Benedikter, F. Ziegler, J. Groos, P. M. Hauser, R. Schowner, M. R. Buchmeiser, *Coord. Chem. Rev.* **2020**, *415*, 213315.
[8] C. Samojłowicz, M. Bieniek, K. Grela, *Chem. Rev.* **2009**, *109*, 3708–3742.
[9] G. C. Vougioukalakis, R. H. Grubbs, *Chem. Eur. J.* **2008**, *14*, 7545–7556.
[10] F. Prencipe, A. Zanfardino, M. Di Napoli, F. Rossi, S. D'Errico, G. Piccialli, G. F. Mangiatordi, M. Saviano, L. Ronga, M. Varcamonti, D. Tesauro, *Int. J. Mol. Sci.* **2021**, *22*, 2497.
[11] Q. Zhao, B. Han, C. Peng, N. Zhang, W. Huang, G. He, J.-L. Li, *Med. Res. Rev.* **2024**, *44*, 2194–2235, DOI 10.1002/med.22039.
[12] I. Ott, in *Adv. Inorg. Chem.* (Eds: P. J. Sadler, R. van Eldik), Academic Press **2020**, 121–148.
[13] H. Clavier, K. Grela, A. Kirschning, M. Mauduit, S. P. Nolan, *Angew. Chem. Int. Ed.* **2007**, *46*, 6786–6801.
[14] M. S. Sanford, J. A. Love, R. H. Grubbs, *J. Am. Chem. Soc.* **2001**, *123*, 6543–6554.
[15] D. J. Nelson, S. Manzini, C. A. Urbina-Blanco, S. P. Nolan, *Chem. Commun.* **2014**, *50*, 10355–10375.
[16] S. P. Nolan, H. Clavier, *Chem. Soc. Rev.* **2010**, *39*, 3305–3316.
[17] M. Scholl, T. M. Trnka, J. P. Morgan, R. H. Grubbs, *Tetrahedron Lett.* **1999**, *40*, 2247–2250.
[18] J. Huang, E. D. Stevens, S. P. Nolan, J. L. Petersen, *J. Am. Chem. Soc.* **1999**, *121*, 2674–2678.
[19] N. Ledoux, B. Allaert, F. Verpoort, *Eur. J. Inorg. Chem.* **2007**, *2007*, 5578–5583.
[20] A. M. Maj, L. Delaude, A. Demonceau, A. F. Noels, *J. Organomet. Chem.* **2007**, *692*, 3048–3056.
[21] P. Csabai, F. Joó, *Organometallics* **2004**, *23*, 5640–5643.
[22] S. P. Shan, X. Xiaoke, B. Gnanaprakasam, T. T. Dang, B. Ramalingam, H. V. Huynh, A. M. Seayad, *RSC Adv.* **2014**, *5*, 4434–4442.
[23] B. S. Murray, M. V. Babak, C. G. Hartinger, P. J. Dyson, *Coord. Chem. Rev.* **2016**, *306*, 86–114.
[24] C. S. Allardyce, P. J. Dyson, D. J. Ellis, S. L. Heath, *Chem. Commun.* **2001**, *0*, 1396–1397.
[25] A. Weiss, R. H. Berndsen, M. Dubois, C. Müller, R. Schibli, A. W. Griffioen, P. J. Dyson, P. Nowak-Sliwinska, *Chem. Sci.* **2014**, *5*, 4742–4748.
[26] G. C. Vougioukalakis, R. H. Grubbs, *Chem. Rev.* **2010**, *110*, 1746–1787.
[27] K. M. Hindi, M. J. Panzner, C. A. Tessier, C. L. Cannon, W. J. Youngs, *Chem. Rev.* **2009**, *109*, 3859–3884.
[28] L. Delaude, A. Demonceau, *Dalton Trans.* **2012**, *41*, 9257–9268.
[29] Y. Kong, S. Xu, H. Song, B. Wang, *Organometallics* **2012**, *31*, 5527–5532.
[30] R. Troiano, C. Costabile, F. Grisi, *Catalysts* **2023**, *13*, 34.
[31] A. Perfetto, C. Costabile, P. Longo, F. Grisi, *Organometallics* **2014**, *33*, 2747–2759.
[32] I. C. Stewart, T. Ung, A. A. Pletnev, J. M. Berlin, R. H. Grubbs, Y. Schrodi, *Org. Lett.* **2007**, *9*, 1589–1592.
[33] C. K. Chung, R. H. Grubbs, *Org. Lett.* **2008**, *10*, 2693–2696.
[34] V. Paradiso, C. Costabile, F. Grisi, *Molecules* **2016**, *21*, 117.
[35] J. DePasquale, M. Kumar, M. Zeller, E. T. Papish, *Organometallics* **2013**, *32*, 966–979.
[36] W. Chen, J. Egly, A. I. Poblador-Bahamonde, A. Maisse-Francois, S. Bellemin-Laponnaz, T. Achard, *Dalton Trans.* **2020**, *49*, 3243–3252.
[37] J. Egly, W. Chen, A. Maisse-François, S. Bellemin-Laponnaz, T. Achard, *Eur. J. Inorg. Chem.* **2022**, *2022*, e202101033.
[38] V. Mechrouk, A. Maisse-François, S. Bellemin-Laponnaz, T. Achard, *Eur. J. Inorg. Chem.* **2023**, *26*, e202300188.
[39] N. Kaloğlu, M. Achard, C. Bruneau, İ. Özdemir, *Eur. J. Inorg. Chem.* **2019**, *2019*, 2598–2606.
[40] M. Yiğit, B. Yiğit, İ. Özdemir, E. Çetinkaya, B. Çetinkaya, *Appl. Organomet. Chem.* **2006**, *20*, 322–327.
[41] D. Yang, Y. Tang, H. Song, B. Wang, *Organometallics* **2015**, *34*, 2012–2017.
[42] L. Delaude, M. Szypa, A. Demonceau, A. F. Noels, *Adv. Synth. Catal.* **2002**, *344*, 749–756.
[43] T. Opstal, K. Couchez, F. Verpoort, *Adv. Synth. Catal.* **2003**, *345*, 393–401.
[44] X. Sauvage, Y. Borguet, A. F. Noels, L. Delaude, A. Demonceau, *Adv. Synth. Catal.* **2007**, *349*, 255–265.
[45] C. Lo, R. Cariou, C. Fischmeister, P. H. Dixneuf, *Adv. Synth. Catal.* **2007**, *349*, 546–550.
[46] T. E. Zehnder, D. J. Nasrallah, J. L. Stanley, J. J. Kiernicki, N. K. Szymczak, C. S. Schindler, *Organometallics* **2023**, *42*, 479–485.

[47] D. S. Müller, Y. Raoul, J. Le Nôtre, O. Baslé, M. Mauduit, *ACS Catal.* **2019**, *9*, 3511–3518.
[48] D. P. Oliveira, T. R. Cruz, D. M. Martins, P. I. S. Maia, A. E. H. Machado, A. L. Bogado, B. E. Goi, B. S. Lima-Neto, V. P. Carvalho-Jr, *Catal. Today* **2021**, *381*, 34–41.
[49] A. D'Amato, A. Mariconda, D. Iacopetta, J. Ceramella, A. Catalano, M. S. Sinicropi, P. Longo, *Pharmaceuticals (Basel)* **2023**, *16*, 1729.
[50] L. Oehninger, H. Alborzinia, S. Ludewig, K. Baumann, S. Wölfl, I. Ott, *ChemMedChem* **2011**, *6*, 2142–2145.
[51] W. Liu, R. Gust, *Chem. Soc. Rev.* **2013**, *42*, 755–773.
[52] A. Casini, C. Gabbiani, F. Sorrentino, M. P. Rigobello, A. Bindoli, T. J. Geldbach, A. Marrone, N. Re, C. G. Hartinger, P. J. Dyson, L. Messori, *J. Med. Chem.* **2008**, *51*, 6773–6781.
[53] R. E. Morris, R. E. Aird, P. del Socorro Murdoch, H. Chen, J. Cummings, N. D. Hughes, S. Parsons, A. Parkin, G. Boyd, D. I. Jodrell, P. J. Sadler, *J. Med. Chem.* **2001**, *44*, 3616–3621.
[54] P. Nowak-Sliwinska, J. R. van Beijnum, A. Casini, A. A. Nazarov, G. Wagnières, H. van den Bergh, P. J. Dyson, A. W. Griffioen, *J. Med. Chem.* **2011**, *54*, 3895–3902.
[55] L. Oehninger, M. Stefanopoulou, H. Alborzinia, J. Schur, S. Ludewig, K. Namikawa, A. Muñoz-Castro, R. W. Köster, K. Baumann, S. Wölfl, W. S. Sheldrick, I. Ott, *Dalton Trans.* **2013**, *42*, 1657–1666.
[56] J. Ceramella, R. Troiano, D. Iacopetta, A. Mariconda, M. Pellegrino, A. Catalano, C. Saturnino, S. Aquaro, M. S. Sinicropi, P. Longo, *Antibiotics* **2023**, *12*, 693.
[57] A. Mariconda, M. Sirignano, C. Costabile, P. Longo, *J. Mol. Catal.* **2020**, *480*, 110570.
[58] M. Sirignano, A. D'Amato, C. Costabile, A. Mariconda, A. Crispini, F. Scarpelli, P. Longo, *Front. Chem.* **2023**, *11*, 1260726.
[59] M. Picq, A. F. Prigent, G. Nemoz, A. C. Andre, H. Pacheco, *J. Med. Chem.* **1982**, *25*, 1192–1198.
[60] G. Lv, L. Guo, L. Qiu, H. Yang, T. Wang, H. Liu, J. Lin, *Dalton Trans.* **2015**, *44*, 7324–7331.
[61] W.-Q. Wang, Y. Yuan, Y. Miao, B.-Y. Yu, H.-J. Wang, Z.-Q. Wang, W. Sang, C. Chen, F. Verpoort, *Appl. Organomet. Chem.* **2020**, *34*, e5323.
[62] H. Cheng, M.-Q. Xiong, C.-X. Cheng, H.-J. Wang, Q. Lu, H.-F. Liu, F.-B. Yao, C. Chen, F. Verpoort, *Chem. Asian J.* **2018**, *13*, 440–448.
[63] J. Ceramella, A. Mariconda, M. Sirignano, D. Iacopetta, C. Rosano, A. Catalano, C. Saturnino, M. S. Sinicropi, P. Longo, *Pharmaceuticals (Basel)* **2022**, *15*, 507.
[64] D. Cirri, S. Pillozzi, C. Gabbiani, J. Tricomi, G. Bartoli, M. Stefanini, E. Michelucci, A. Arcangeli, L. Messori, T. Marzo, *Dalton Trans.* **2017**, *46*, 3311–3317.
[65] A. Demonceau, A. F. Noels, E. Saive, A. J. Hubert, *J. Mol. Catal.* **1992**, *76*, 123–132.
[66] L. Delaude, A. Demonceau, A. F. Noels, *Curr. Org. Chem.* **2006**, *10*, 203–215.
[67] J. Baran, I. Bogdanska, D. Jan, L. Delaude, A. Demonceau, A. F. Noels, *J. Mol. Catal. Chem.* **2002**, *190*, 109–116.
[68] F. Quintin, J. Pinaud, F. Lamaty, X. Bantreil, *Organometallics* **2020**, *39*, 636–639.
[69] J. Chen, X. Chen, C. Zhu, J. Zhu, *J. Mol. Catal. Chem.* **2014**, *394*, 198–204.
[70] M. Picq, A. F. Prigent, G. Nemoz, A. C. Andre, H. Pacheco, *J. Med. Chem.* **1982**, *25*, 1192–1198.
[71] D. Cirri, S. Pillozzi, C. Gabbiani, J. Tricomi, G. Bartoli, M. Stefanini, E. Michelucci, A. Arcangeli, L. Messori, T. Marzo, *Dalton Trans.* **2017**, *46*, 3311–3317.
[72] J. Ceramella, A. Mariconda, C. Rosano, D. Iacopetta, A. Caruso, P. Longo, M. S. Sinicropi, C. Saturnino, *ChemMedChem* **2020**, *15*, 2306–2316.
[73] D. Iacopetta, C. Rosano, M. Sirignano, A. Mariconda, J. Ceramella, M. Ponassi, C. Saturnino, M. S. Sinicropi, P. Longo, *Pharmaceuticals* **2020**, *13*, 91.

Manuscript received: June 26, 2024
Revised manuscript received: August 13, 2024
Accepted manuscript online: August 16, 2024
Version of record online: October 17, 2024